Photometry of Centaurs and trans-Neptunian objects: 2060 Chiron (1977 UB), 10199 Chariklo (1997 CU_{26}), 38628 Huya (2000 EB_{173}), 28978 Ixion (2001 KX_{76}), and 90482 Orcus (2004 DW)

M. Galiazzo • C. de la Fuente Marcos • R. de la Fuente Marcos • G. Carraro[1] • M. Maris • M. Montalto

Abstract Both Centaurs and trans-Neptunian objects (TNOs) are minor bodies found in the outer Solar System. Centaurs are a transient population that moves between the orbits of Jupiter and Neptune, and they probably diffused out of the TNOs. TNOs move mainly beyond Neptune. Some of these objects display episodic cometary behaviour; a few percent of them are known to host binary companions. Here, we study the light-curves of two Centaurs —2060 Chiron (1977 UB) and 10199 Chariklo (1997 CU_{26})— and three TNOs —38628 Huya (2000 EB_{173}), 28978 Ixion (2001 KX_{76}), and 90482 Orcus (2004 DW)— and the colours of the Centaurs and Huya. Precise, ∼1%, R-band absolute CCD photometry of these minor bodies acquired between 2006 and 2011 is presented; the new data are used to investigate the rotation rate of these objects. The colours of the Centaurs and Huya are determined using $BVRI$ photometry. The point spread function of the five minor bodies is analysed, searching for signs of a coma or close companions. Astrometry is also discussed. A periodogram analysis of the light-curves of these objects gives the following rotational periods: 5.5±0.4 h for Chiron, 7.0±0.6 h for Chariklo, 4.45±0.07 h for Huya, 12.4±0.3 h for Ixion, and 11.9±0.5 h for Orcus. The colour indices of Chiron are found to be $B-V = 0.53 \pm 0.05$, $V-R = 0.37 \pm 0.08$, and $R-I = 0.36 \pm 0.15$. The values computed for Chariklo are $V-R = 0.62 \pm 0.07$ and $R-I = 0.61 \pm 0.07$. For Huya, we find $V-R = 0.58 \pm 0.09$ and $R-I = 0.64 \pm 0.20$. Our rotation periods are similar to and our colour values are consistent with those already published for these objects. We find very low levels of cometary activity (if any) and no sign of close or wide binary companions for these minor bodies.

Keywords Minor planets, asteroids: individual: 2060 Chiron (1977 UB) · Minor planets, asteroids: individual: 10199 Chariklo (1997 CU_{26}) · Minor planets, asteroids: individual: 38628 Huya (2000 EB_{173}) · Minor planets, asteroids: individual: 28978 Ixion (2001 KX_{76}) · Minor planets, asteroids: individual: 90482 Orcus (2004 DW) · Techniques: photometric

M. Galiazzo

Department of Physics and Astronomy, The University of Western Ontario, London, ON N6A 3K7, Canada

C. de la Fuente Marcos

R. de la Fuente Marcos

Apartado de Correos 3413, E-28080 Madrid, Spain

G. Carraro

European Southern Observatory, Alonso de Cordova 3107, Casilla 19001, Santiago 19, Chile

M. Maris

INAF, Osservatorio Astronomico di Trieste, via G.B. Tiepolo 11, I-34131, Trieste, Italy

M. Montalto

Centro de Astrofísica da Universidade do Porto, (CAUP), P-4150-762 Porto, Portugal

[1]Dipartimento di Fisica e Astronomia, Università degli Studi di Padova, Vicolo dell'Osservatorio 3, I-35122, Padova, Italy.

1 Introduction

Centaurs are a group of minor planets found in the outer Solar System whose orbits are strongly perturbed as a result of crossing the paths of one or more of the giant planets (Di Sisto & Brunini 2007; Galiazzo et al. 2015). Objects in this dynamical class are widely thought to be former members of the so-called Trans-Neptunian Belt (TNB; e.g. Jewitt & Luu 1993) or even the Oort Cloud (Levison et al. 2001), and some of them may be transitioning to become short-period comets (e.g. Levison & Duncan 1997). However, the possible existence of trans-Plutonian planets (see e.g. Trujillo & Sheppard 2014; de la Fuente Marcos & de la Fuente

Marcos 2014; de la Fuente Marcos et al. 2015; Batygin & Brown 2016) may affect the dynamical pathways leading to this dynamical class. This transient population features perihelia of less than 30 AU, but outside the orbit of Jupiter. A number of them display episodic cometary behaviour (e.g. Jewitt 2009). Trans-Neptunian objects (TNOs) inhabit the TNB and their semi-major axes lie beyond that of Neptune. TNOs actively engaged in mean-motion resonances with Neptune are believed to have become trapped there during planet migration, late in the giant-planet formation process (e.g. Gladman et al. 2012). Issues of nomenclature in the outer Solar System are discussed by e.g. Gladman et al. (2008). A few percent of both Centaurs and TNOs are known to host binary companions (e.g. Walsh 2009; Naoz et al. 2010; Parker 2011; Parker et al. 2011).

In this paper, we present new photometric data of two Centaurs —2060 Chiron (1977 UB) and 10199 Chariklo (1997 CU_{26})— and three TNOs —38628 Huya (2000 EB_{173}), 28978 Ixion (2001 KX_{76}), and 90482 Orcus (2004 DW). The observations are part of a programme focused on the study of Centaurs, TNOs, and their possible cometary activity. Observations and data processing techniques are described in Sect. 2. Chiron is revisited in Sect. 3. New data and results for Chariklo are presented in Sect. 4. Those for TNOs Huya, Ixion, and Orcus are given in Sects. 5–7, respectively. Results are discussed and conclusions summarised in Sect. 8.

2 Observations and data reduction

The observations presented here were acquired at the Las Campanas Observatory, between 2006 and 2011, using the 1.0-m Swope telescope equipped with the site#3 2048 × 3150 CCD camera. In the frames, the field of view is about $14'.8 \times 22'.8$ and the pixel scale is $0.435''$/pixel. Preliminary processing of the CCD frames was carried out using standard routines of the IRAF package.[1] Both dome and sky flat-field frames were obtained in each filter ($BVRI$) as needed and the images were also corrected for non-linearity (Hamuy et al. 2006; Carraro 2009); additional details can be found in Galiazzo (2009). Photometric calibration of the targets including appropriate zero points and color terms computed for the individual observing nights —when photometric— was performed. As an example, the following relationships between the instrumental (lower-case letters) and the standard colours and magnitudes were adopted in the case of Chariklo (see Sect. 4):

$$
\begin{aligned}
V &= 22.115(0.004) + v - 0.068(0.007) \times (B - V) \\
&\quad + 0.16(0.02) \times X \,, \qquad (1) \\
B &= 22.084(0.004) + b + 0.054(0.007) \times (B - V) \\
&\quad + 0.30(0.02) \times X \,, \qquad (2) \\
I &= 22.179(0.006) + i + 0.058(0.009) \times (V - I) \\
&\quad + 0.06(0.02) \times X \,, \qquad (3)
\end{aligned}
$$

where X is the airmass and the values of the errors associated with the various coefficients appear in parentheses. These expressions were derived merging together standard stars from three different photometric nights after checking that their apparent brightnesses were stable. Second order color terms were computed, but turned out to be negligible. Astrometric calibration of the CCD frames was performed using the algorithms of the *Astrometry.net* system (Lang et al. 2010). In the data tables presented here, when no magnitude is provided for a given astrometric entry (see Appendix A), it means that it was not computed because of the low quality of the CCD frame or the presence of stars too close (even partially or completely blended with it) to the photometric target. Due to the sparse nature of our data, period determination is made using one of the string-length period search algorithms, the Lafler-Kinman method (Lafler & Kinman 1965; Clarke 2002). String-length methods are better suited for this task when only a small number of randomly spaced observations are available (e.g. Dworetsky 1983). False alarm probabilities are evaluated using the Bootstrap method (e.g. Press et al. 2007) with 500 trials.

3 2060 Chiron (1977 UB)

Discovered in 1977, Chiron is the first known Centaur and one of the largest; its diameter amounts to 218±20 km, with an albedo of 16±3% (Fornasier et al. 2013). The rotational period of Chiron as determined by Bus et al. (1989), Marcialis & Buratti (1993) or Sheppard et al. (2008) amounts to 5.9178 h, but Fornasier et al. (2013) have found a value of 5.40±0.03 h in December 2011, with an amplitude equal to 0.06–0.07 mag. This Centaur shows cometary activity (e.g. Luu & Jewitt 1990) and it may have a ring (Ortiz et al. 2015; Ruprecht et al. 2015). Because of this cometary activity, its absolute magnitude changes over time (Belskaya et al. 2010). $BVRI$ photometry of Chiron was

[1] IRAF is distributed by the National Optical Astronomy Observatory, which is operated by the Association of Universities for Research in Astronomy (AURA) under a cooperative agreement with the National Science Foundation.

obtained in 2006 June and again in 2011 July–August (but only in R) using the same equipment.

During the first observing run (2006 June 26 to 30), Chiron was in Capricornus; as the object's apparent sky motion during the observations was 0.11″/minute and the exposure time was 400 s, the expected shift during one exposure was well within the seeing disk ($1\farcs20$). The average geocentric distance of Chiron during the observing run was $\bar{\Delta}$=13.32 AU, the average heliocentric distance was $\bar{r}$=14.18 AU, and the average phase angle (Earth-Chiron-Sun angle) was $\bar{\alpha}=2\fdg3$. Table 1 includes the values of the apparent magnitude (Mag) and its associated error ($\pm\sigma$) at the appropriate UT-time (Julian date), the filter used, the airmass (A.M.) and the solar phase angle α in degrees; the associated astrometry is in Table 9. In this and subsequent calculations the errors quoted correspond to one standard deviation (1σ) computed applying the usual expressions (see e.g. Wall & Jenkins 2012). A total of 25 frames obtained in R and one in each of the B, V, R, and I filters are presented in Table 1.

The periodogram corresponding to the first run is shown in Fig. 1, middle panel. Our best fitting gives a rotational period $P = 5.5 \pm 0.4$ h (or a frequency of 0.183±0.014 rotations per hour). The values of the false alarm probabilities are relatively low: the probability that there is no period with value P is 1.6±0.6% and that of the observations containing a period that is different from P is <0.01%. The light-curve of Chiron in Fig. 1, bottom panel, shows the detrended data (by fitting a linear function to the data and subtracting) from the top panel phased with the best-fit period, its amplitude is ∼0.1 mag. Its light-curve amplitude was found to be 0.088 mag in 1986 and 1988 (Bus et al. 1989) and 0.044 mag in 1991 (Marcialis & Buratti 1993), but it was measured at 0.003±0.015 mag with data obtained in 2013 (Ortiz et al. 2015). The raw data in Fig. 1 show a dimming trend that amounts to about 0.1 mag. Raw lightcurves often exhibit smooth trends with timescales of a few days. In our case (see also Figs. 2 and 3), the smooth component seems to be roughly piecewise linear. There are multiple reasons for this behaviour, including seeing-induced variability. It may also be intrinsic to the object under study. For example, fig. 6(a) in Luu & Jewitt (1990) shows Chiron's rotational variations superposed on a linear brightening trend and this could not be attributed to errors in the correction for atmospheric extinction; Chiron naturally exhibits short-term brightness variations (on timescales of hours). Luu & Jewitt (1990) removed the linear trend in their fig. 6(b) to facilitate their subsequent rotational period analysis; the brightening trend amounted to about 0.12 mag which is consistent with our Fig. 1, although in our case we observe dimming not brightening.

Unfortunately, our sparse curve does not sample the entire rotational period well and this may explain why our value of P is somewhat smaller than the ones measured by other authors (i.e. Sheppard et al. 2008), although the accepted value is nearly within 1σ. However, it matches well the recent determination in Fornasier et al. (2013); the value of our amplitude is also consistent with theirs. The value of the absolute magnitude in V derived by Fornasier et al. (2013) is 5.80±0.04 mag; ours is 5.75±0.06 mag which again is compatible with theirs and also with the mean value found over 2004–2008 (see fig. 2 in Fornasier et al. 2013). The absolute magnitude in V has been computed using eqs. (1) and (2) in Romanishin & Tegler (2005).

Our photometric data are compatible with a negligible level of cometary activity at the time of the observations and we found no evidence for a comoving (close or wide) companion (see Sect. 8 for additional details). Regarding the colours of this object, we only used consecutive images, or almost consecutive, on the $BVRI$ filters. Adopting this approach we avoid errors induced by possible rotational variability associated with surface features. The colour indices of Chiron were found to be $B - V = 0.53 \pm 0.05$, $V - R = 0.37 \pm 0.08$, and $R - I = 0.36 \pm 0.15$. Our values are consistent with those already published for this object (e.g. Hainaut & Delsanti 2002; Barucci et al. 2005).

Chiron was reobserved from 2011 July 30 to August 6 (see Tables 2 and 10). The average geocentric distance of Chiron during this second observing run was $\bar{\Delta}$=15.92 AU, the average heliocentric distance was $\bar{r}$=16.84 AU, and the average phase angle was $\bar{\alpha}=1\fdg5$. Unfortunately, the nights were not photometric and the seeing was variable and worse than that of the first run. Apparent magnitudes in Table 2 are relative to two suitable reference field stars (not known variables) close to the target body. An additional, exploratory observing run for Chiron was carried out with the Cerro Tololo InterAmerican Observatory SMARTS 1-m telescope and Y4kCam on 2006 May 19 to 22 (see Table 11). During this initial observing run only astrometry was obtained. The average geocentric distance of Chiron was $\bar{\Delta}$=13.74 AU, the average heliocentric distance was $\bar{r}$=14.11 AU, and the average phase angle was $\bar{\alpha}=3\fdg9$.

4 10199 Chariklo (1997 CU_{26})

Currently the largest confirmed Centaur, Chariklo has a rotational period of 7.00±0.04 h, an effective radius

Table 1 Photometry of 2060 Chiron (1977 UB); 2006 June. This table includes the values of the apparent magnitude (Mag) and its associated error ($\pm\sigma$) at the appropriate UT-time (Julian date), the filter used, the airmass (A.M.) and the solar phase angle α in degrees.

Julian date	Filter	A.M.	Exp. (s)	Mag	α (°)
2453912.805822	R	1.05	400	16.921±0.023	2.36
2453912.824410	R	1.07	400	16.932±0.026	2.36
2453912.857975	R	1.13	400	16.936±0.035	2.35
2453912.864005	R	1.15	400	16.924±0.024	2.35
2453912.870023	R	1.16	400	16.908±0.032	2.35
2453912.876053	R	1.19	400	16.954±0.022	2.35
2453912.882083	R	1.21	400	16.935±0.021	2.35
2453912.897037	R	1.28	400	16.981±0.021	2.35
2453912.903067	R	1.31	400	16.996±0.021	2.35
2453914.689248	R	1.28	400	17.014±0.017	2.25
2453914.695278	R	1.25	400	17.065±0.019	2.25
2453914.701296	R	1.22	400	17.091±0.021	2.25
2453914.724491	R	1.14	400	17.066±0.014	2.25
2453914.730521	R	1.13	400	17.046±0.014	2.25
2453914.736539	R	1.11	400	17.074±0.011	2.25
2453914.758970	R	1.07	400	17.061±0.012	2.24
2453914.765000	R	1.07	400	17.070±0.038	2.24
2453914.771030	R	1.06	400	17.030±0.017	2.24
2453914.777049	R	1.06	400	17.040±0.017	2.24
2453914.783079	R	1.05	400	17.032±0.018	2.24
2453914.789167	R	1.05	400	17.035±0.021	2.24
2453914.794502	R	1.05	400	17.012±0.013	2.24
2453914.801227	R	1.05	400	17.008±0.027	2.24
2453914.807245	R	1.06	400	17.076±0.059	2.24
2453914.813275	R	1.06	400	17.117±0.025	2.24
2453912.798391	B	1.05	600	17.815±0.025	2.36
2453912.811991	V	1.06	400	17.287±0.026	2.36
2453912.818206	I	1.06	400	16.564±0.590	2.36

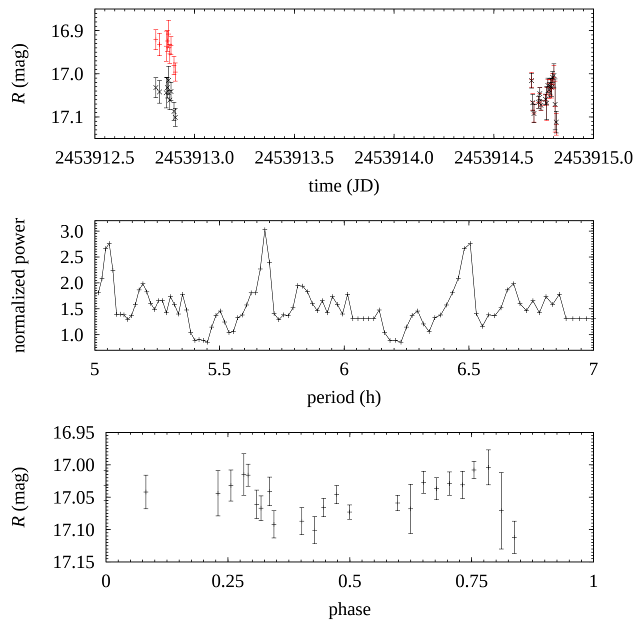

Fig. 1 Chiron: 2006 June 26–30 run. R-band data, raw (red) and detrended (black), but uncorrected for rotational variation, used to compute the rotation period of Chiron (top panel). Lafler-Kinman periodogram of Chiron (middle panel) using 4×25 test frequencies. Periods yielding the lowest normalized power are the most likely, statistically speaking. The lowest value corresponds to a rotation period of 5.5±0.4 h or a frequency of 0.183±0.014 cycles/h with a false alarm probability (500 trials, see the text) of 1.6%. Rotational light-curve of Chiron phased to a period of 5.5 hours (bottom panel).

Table 2 Photometry of 2060 Chiron (1977 UB); 2011 July–August. All the observations in the R filter; notation as in Table 1.

Julian date	A.M.	Exp. (s)	Mag	α (°)
2455772.717766	1.17	600	19.557±0.075	1.64
2455772.726655	1.15	600	19.370±0.061	1.64
2455772.738704	1.13	800	18.210±0.027	1.64
2455772.750451	1.12	800	17.233±0.011	1.64
2455772.761412	1.11	800	17.325±0.012	1.64
2455772.772199	1.10	800	16.899±0.008	1.64
2455772.783102	1.11	800	16.864±0.007	1.64
2455772.793854	1.11	800	16.864±0.008	1.63
2455772.804618	1.12	800	16.875±0.008	1.63
2455772.815347	1.14	800	16.866±0.008	1.63
2455772.829167	1.17	800	16.869±0.008	1.63
2455772.840347	1.20	800	17.156±0.009	1.63
2455772.850046	1.24	600	17.347±0.011	1.63
2455772.858657	1.27	600	17.202±0.010	1.63
2455772.867060	1.32	600	17.197±0.010	1.63
2455772.875475	1.36	600	17.188±0.010	1.63
2455772.883889	1.42	600	17.190±0.010	1.63
2455772.892292	1.48	600	17.191±0.010	1.63
2455772.900706	1.56	600	17.227±0.010	1.63
2455772.909144	1.64	600	17.202±0.011	1.63
2455775.694271	1.22	600	17.714±0.015	1.48
2455775.702766	1.19	600	19.942±0.117	1.48
2455775.712813	1.16	600	19.013±0.049	1.48
2455775.723380	1.14	900	19.542±0.097	1.48
2455775.746100	1.11	900	18.439±0.034	1.48
2455775.758449	1.11	900	17.691±0.020	1.48
2455775.770694	1.10	900	16.889±0.008	1.48
2455775.792616	1.12	900	16.938±0.009	1.48
2455775.805799	1.14	900	16.718±0.007	1.48
2455775.816470	1.16	600	17.972±0.020	1.48
2455775.860116	1.33	600	17.992±0.020	1.47
2455775.871898	1.39	600	17.700±0.016	1.47
2455775.880336	1.46	600	17.546±0.013	1.47
2455775.888762	1.53	600	17.591±0.015	1.47
2455775.897187	1.61	600	17.265±0.011	1.47
2455775.905613	1.70	600	17.464±0.014	1.47
2455775.914039	1.82	600	17.210±0.011	1.47
2455779.679375	1.23	600	17.099±0.011	1.27
2455779.687778	1.20	600	17.109±0.011	1.27
2455779.697523	1.17	600	17.076±0.010	1.27
2455779.705926	1.15	600	17.033±0.010	1.27
2455779.714317	1.14	600	16.623±0.006	1.27
2455779.722847	1.12	600	16.808±0.008	1.27
2455779.731238	1.11	600	17.138±0.028	1.27
2455779.765116	1.11	600	17.047±0.059	1.26
2455779.773600	1.11	600	16.797±0.007	1.26
2455779.781991	1.12	600	17.099±0.011	1.26
2455779.790394	1.13	600	17.092±0.009	1.26
2455779.814792	1.18	900	16.856±0.010	1.26
2455779.825417	1.22	600	17.123±0.010	1.26
2455779.833854	1.25	600	17.108±0.010	1.26
2455779.842245	1.29	600	17.099±0.009	1.26
2455779.850694	1.34	600	17.134±0.010	1.26
2455779.859097	1.39	600	17.231±0.010	1.26
2455779.867488	1.44	600	17.138±0.009	1.26
2455779.876146	1.51	600	17.113±0.009	1.26
2455779.884560	1.59	600	17.140±0.009	1.26
2455779.893032	1.69	600	17.144±0.010	1.26
2455779.901435	1.80	600	17.133±0.010	1.26

of 119±5 km (Fornasier et al. 2014), and a dense ring system (Braga-Ribas et al. 2014; Duffard et al. 2014). Due to the rings, the average value of the albedo, 4.2% (Fornasier et al. 2014), is variable (Duffard et al. 2014). VRI photometry of Chariklo was obtained in 2006 June and again in 2011 July–August using the same equipment. During the first observing run, Chariklo was in Hydra and the observations were completed during 5 nights, 3 (2006 June 26, 28 and 29) of them photometric. During the second run, that lasted 6 nights, Chariklo was in Lupus. These nights were not photometric and only frames in the R-band were collected.

For the first observing run, preliminary processing of the CCD frames was made as described in Sect. 2. The average seeing was $1\farcs20$ along the entire 5 nights run (2006 June 26 to 30). The sky motion of Chariklo during this first run was $0.071''$/minute and the typical exposure time was 400 s; therefore, the expected shift within a given image is again well within the seeing disk. The average geocentric distance of Chariklo during the observing run was $\bar{\Delta} = 12.98$ AU, the average heliocentric distance was $\bar{r}$=13.20 AU, and the average phase angle (Earth–Chariklo–Sun angle) was $\bar{\alpha} = 4\fdg35$. On each of the photometric nights, we observed 96 standard stars extracted from repeated observations of the four fields Mark A, PG 1657, PG 2213 and SA 110 (Landolt 1992) at different airmasses. Aperture photometry of standard stars was obtained with an aperture radius of $6\farcs09$ (14 pixels). The instrumental photometry of Chariklo and several field stars was extracted with the DAOPHOTII (Stetson 1987) package, with a fitting radius of 5 pixels. We used five stable field stars as reference to shift Chariklo's magnitudes to the first night (June 27th), which was photometric. We then estimated aperture corrections for the field stars, that we applied to Chariklo's measurements —see Carraro et al. (2006) and Galiazzo (2009) for further details. This correction turned out to be smaller than 0.10 mag in all filters. Table 3 is analogous in structure to Table 1 and includes Chariklo's data details for the 2006 run; the associated astrometry can be found in Table 12. The data are plotted in Fig. 2, top panel.

The periodogram for the first run (Fig. 2, middle panel) shows a broad minimum between 6.8 and 7.3 h. Our best fit for the rotational period is $P = 7.0 \pm 0.6$ h (or a frequency of 0.142±0.013 rotations per hour). The probability that there is no period with value P is 4.2±0.9% and that of the observations containing a period that is different from P is 0.2±0.2%. The lightcurve of Chariklo in Fig. 2, bottom panel, represents the detrended data from the top panel phased with the best-fit period. Our sparse curve matches well that in fig. 1 of Fornasier et al. (2014), which has an amplitude of 0.11 mag: it displays asymmetric double peaks and an amplitude of $\sim$0.13 mag. The amplitude in Lacerda & Luu (2006) is about 0.1 mag. The rings affect the amplitude of the overall rotational light-curve as their aspect angle changes over time (Duffard et al. 2014). The value of the absolute magnitude in V found by Fornasier et al. (2014) is 7.03$\pm$0.10 mag; our determination (found as described in Sect. 3), 7.24$\pm$0.08 mag, is compatible with this value. Consistently with results in Fornasier et al. (2014) and Duffard et al. (2014) no coma was detected (but see Sect. 8 for additional details).

Regarding the colour indices, the values found for Chariklo were $B-V = 0.80 \pm 0.05$, $V-R = 0.62 \pm 0.07$, and $R-I = 0.61 \pm 0.07$. Again, the values are consistent with some already published for this object (e.g. Hainaut & Delsanti 2002). However, they are different from those in Fulchignoni et al. (2008): $V-R = 0.48$, $V-I = 1.01$. These significant differences may be the result of changes in the appearance of the rings that induce variations in the overall spectral properties of this object as the absorption band due to water ice disappears when the rings are edge-on (Duffard et al. 2014; Fornasier et al. 2014).

Conditions during the second run were less favourable with the seeing changing in the range 1$''$.2–2$''$.0. No standard stars were used in this case. As the nights were not photometric, no attempt is made to calibrate with respect to standards (see Tables 4 and 13). Apparent magnitudes in Table 4 are relative to two suitable reference field stars (not known variables) close to the target body. The average geocentric distance of Chariklo during this second observing run was $\bar{\Delta}$=13.72 AU, the average heliocentric distance was $\bar{r}$=14.08 AU, and the average phase angle was $\bar{\alpha}$=3°.9.

Table 3 Photometry of 10199 Chariklo (1997 CU_{26}); 2006 June. Notation as in Table 1.

Julian date	Filter	A.M.	Exp. (s)	Mag	α (°)
2453914.450405	R	1.00	300	18.011$\pm$0.050	4.34
2453914.462315	R	1.00	400	18.115$\pm$0.017	4.34
2453914.474676	R	1.01	400	18.076$\pm$0.012	4.34
2453914.487072	R	1.02	400	18.093$\pm$0.021	4.34
2453914.539294	R	1.14	400	18.147$\pm$0.027	4.34
2453914.545313	R	1.16	400	18.177$\pm$0.021	4.34
2453914.578819	R	1.32	400	18.154$\pm$0.026	4.34
2453914.584850	R	1.36	400	18.166$\pm$0.020	4.34
2453914.617986	R	1.65	400	18.076$\pm$0.030	4.34
2453915.473970	R	1.01	400	18.196$\pm$0.048	4.35
2453915.489641	R	1.03	400	18.118$\pm$0.053	4.35
2453916.453565	R	1.00	400	18.264$\pm$0.028	4.36
2453916.458426	R	1.00	400	18.301$\pm$0.018	4.36
2453916.463299	R	1.01	400	18.261$\pm$0.016	4.36
2453916.510891	R	1.07	400	18.178$\pm$0.033	4.36
2453916.535081	R	1.14	400	18.179$\pm$0.020	4.36
2453916.560914	R	1.25	400	18.209$\pm$0.023	4.37
2453916.586921	R	1.40	500	18.239$\pm$0.015	4.37
2453916.613403	R	1.65	500	18.257$\pm$0.017	4.37
2453914.456100	V	1.00	400	18.677$\pm$0.024	4.34
2453914.468484	V	1.01	400	18.709$\pm$0.027	4.34
2453914.480833	I	1.01	400	17.542$\pm$0.018	4.34

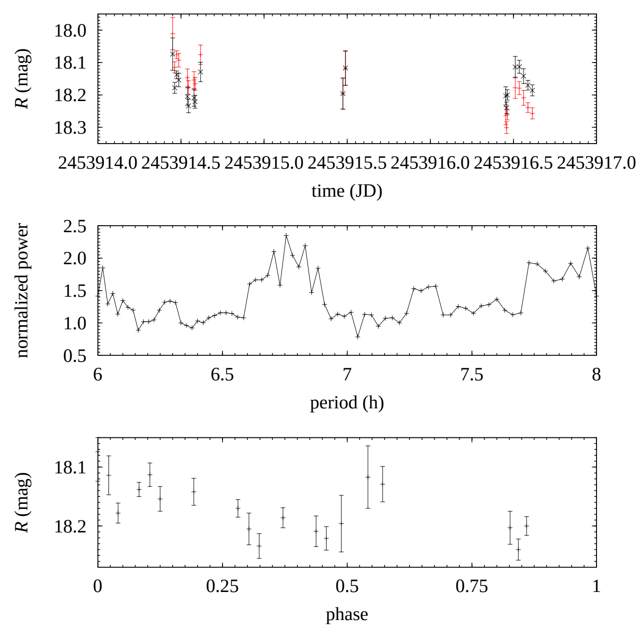

Fig. 2 Same as Fig. 1 but for Chariklo; 4×19 test frequencies. The lowest value of the normalized power corresponds to a rotation period of 7.0$\pm$0.6 h or a frequency of 0.142$\pm$0.013 cycles/h with a false alarm probability < 4.5%. The bottom panel shows the rotational light-curve of Chariklo phased to a period of 7.0 hours.

5 38628 Huya (2000 EB_{173})

Huya is a TNO trapped in a 3:2 mean motion resonance with Neptune, it is therefore a Plutino. Its diameter could be as large as 458$\pm$9 km, with an albedo of 8.3$\pm$0.4% (Fornasier et al. 2013). Thirouin et al. (2014) give a value of 5.28 h for the rotational period of this object; Ortiz et al. (2003) derived a value of 6.75 h. Huya was observed with Chiron and Chariklo in 2006 June (see Tables 5 and 14); it was in Virgo. The average geocentric distance of Huya during the observing run was $\bar{\Delta}$ = 28.59 AU, the average heliocentric distance was $\bar{r}$=29.03 AU, and the average phase angle (Earth–Huya–Sun angle) was $\bar{\alpha}$ = 1°.8. The periodogram in Fig. 3, middle panel, shows several minima. Our best fit for the rotational period is P = 4.45$\pm$0.07 h (or a

Table 4 Photometry of 10199 Chariklo (1997 CU_{26}); 2011 July-August. All the observations in the R filter.

Julian date	A.M.	Exp. (s)	Mag	α (°)
2455772.543628	1.05	600	18.317±0.013	3.83
2455772.584763	1.14	800	18.523±0.232	3.83
2455772.600174	1.20	800	18.321±0.047	3.83
2455772.611632	1.24	800	18.282±0.029	3.83
2455772.622697	1.29	800	18.243±0.040	3.83
2455772.634063	1.36	800	18.284±0.030	3.83
2455772.645208	1.43	800	18.312±0.054	3.83
2455772.656111	1.51	800	18.518±0.138	3.83
2455775.527824	1.04	600	18.286±0.018	3.90
2455775.536250	1.06	600	18.249±0.037	3.90
2455775.553137	1.09	600	18.259±0.021	3.90
2455775.561562	1.11	600	18.246±0.020	3.90
2455775.569988	1.13	600	18.213±0.018	3.90
2455775.578426	1.15	600	18.215±0.024	3.90
2455775.586863	1.18	600	18.225±0.023	3.90
2455775.595289	1.21	600	18.240±0.020	3.90
2455775.603727	1.25	600	18.210±0.020	3.90
2455775.616771	1.31	600	18.185±0.021	3.90
2455775.626400	1.37	600	18.205±0.020	3.90
2455775.670139	1.74	600	18.267±0.019	3.90
2455775.678553	1.85	600	18.249±0.020	3.90
2455778.509792	1.03	600	18.234±0.026	3.95
2455778.518194	1.04	600	18.264±0.028	3.95
2455778.526620	1.05	600	18.256±0.023	3.95
2455778.536684	1.07	600	18.266±0.029	3.95
2455778.545590	1.09	600	18.262±0.022	3.95
2455778.573171	1.16	600	18.301±0.019	3.95
2455778.581586	1.19	600	18.300±0.024	3.95
2455778.619340	1.37	600	18.307±0.020	3.95
2455778.627755	1.43	600	18.277±0.020	3.95
2455778.636169	1.49	600	18.270±0.018	3.95
2455778.644676	1.57	600	18.226±0.019	3.95
2455778.653090	1.65	600	18.226±0.020	3.95

frequency of 0.225±0.003 rotations per hour). This is close to one of the aliases in Thirouin et al. (2014), 4.31 h. The probability that there is no period with value P is 32.5±2.1% and that of the observations containing a period that is different from P is 1.0±0.4%. The light-curve of Huya in Fig. 3, bottom panel, represents the detrended data from the top panel phased with the best-fit period. Our sparse curve looks similar to that in fig. 11 of Thirouin et al. (2014), its amplitude is ~0.1 mag. For Huya, we found the following values of the colours: $B-V = 1.00 \pm 0.06$, $V-R = 0.58 \pm 0.09$, and $R-I = 0.64 \pm 0.20$. These are compatible with those in e.g. Hainaut & Delsanti (2002).

6 28978 Ixion (2001 KX_{76})

Ixion is also a Plutino, one of the largest known. Lellouch et al. (2013) give a value of the diameter of 617±20 km, with an albedo of 14.1±1.1%. A rotational period of 15.9 h has been derived by Rousselot & Petit (2010). Ixion was observed in 2010 May (see Tables 6 and 15) when the object was in Ophiuchus with the same equipment used for the previous three objects. The average geocentric distance of Ixion during the observing run was $\bar{\Delta}$ = 40.48 AU, the average heliocentric distance was $\bar{r}$=41.38 AU, and the average phase angle (Earth–Ixion–Sun angle) was $\bar{\alpha} = 0\overset{\circ}{.}6$. The periodogram in Fig. 4, middle panel, shows several minima. Our best fit for the rotational period is P = 12.4±0.3 h (or a frequency of 0.080±0.002 rotations per hour). The light-curve is rather flat and the error bars are nearly as large as the purported photometric amplitude. The probability that there is no period with value P is 1.2±0.5% and that of the observations containing a period that is different from P is <0.01%. The light-curve of Ixion in Fig. 4, bottom panel, represents the detrended data from the top panel phased with the best-fit period. Unfortunately, the data sampling was rather incomplete. No evidence of cometary activity was found in our CCD frames; this result is consistent with those from previous studies (e.g. Lorin & Rousselot 2007). Ixion was also observed in 2006 (see Table 16), but no useful data were acquired other than astrometry. The average geocentric distance of Ixion during this previous observing run was $\bar{\Delta}$=41.34 AU, the average heliocentric distance was $\bar{r}$=42.25 AU, and the average phase angle was $\bar{\alpha}=0\overset{\circ}{.}6$.

7 90482 Orcus (2004 DW)

Also a Plutino, Orcus is the largest of the objects studied in this paper. Its diameter amounts to 917±25 km

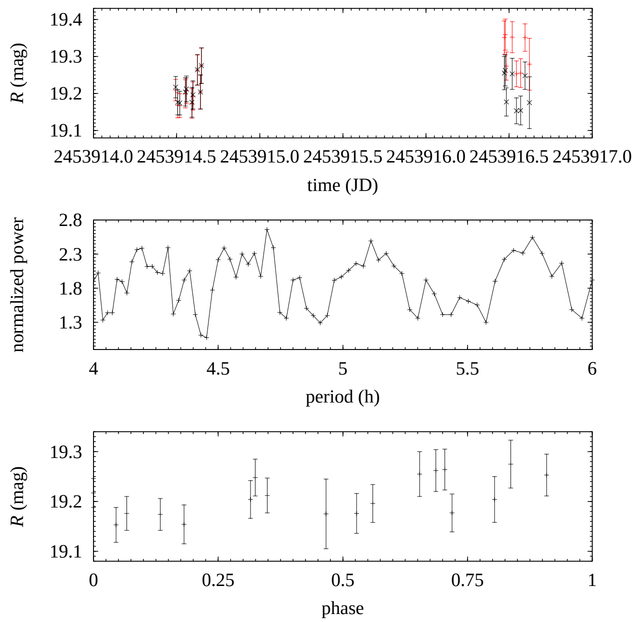

Fig. 3 Same as Fig. 1 but for Huya; 4×18 test frequencies. The lowest value of the normalized power corresponds to a rotation period of 4.45±0.07 h or a frequency of 0.225±0.003 cycles/h with a false alarm probability $< 33\%$. The bottom panel shows the rotational light-curve of Huya phased to a period of 4.45 h.

Table 5 Photometry of 38628 Huya (2000 EB_{173}); 2006 June. Notation as in Table 1.

Julian date	Filter	A.M.	Exp. (s)	Mag	α (°)
2453914.494178	R	1.15	400	19.209±0.029	1.82
2453914.506551	R	1.14	400	19.168±0.034	1.82
2453914.519028	R	1.13	400	19.167±0.032	1.82
2453914.552604	R	1.15	400	19.199±0.038	1.82
2453914.558831	R	1.15	400	19.207±0.035	1.82
2453914.592060	R	1.24	400	19.173±0.040	1.82
2453914.598079	R	1.26	400	19.193±0.038	1.82
2453914.624873	R	1.39	400	19.263±0.041	1.82
2453914.643403	R	1.53	400	19.204±0.046	1.82
2453914.649433	R	1.59	400	19.275±0.048	1.82
2453916.471181	R	1.18	400	19.351±0.045	1.84
2453916.477211	R	1.17	400	19.359±0.042	1.84
2453916.483241	R	1.16	400	19.274±0.038	1.84
2453916.518438	R	1.13	500	19.352±0.042	1.84
2453916.543808	R	1.14	600	19.253±0.035	1.84
2453916.569086	R	1.18	600	19.255±0.039	1.84
2453916.595590	R	1.26	600	19.351±0.037	1.85
2453916.621944	R	1.40	600	19.279±0.070	1.85
2453916.663704	R	1.63	600	20.790±0.578	1.85
2453914.500347	V	1.14	400	19.784±0.023	1.82
2453914.631030	V	1.43	400	19.791±0.029	1.82
2453914.512812	I	1.13	400	18.575±0.028	1.82
2453914.637211	I	1.48	400	18.564±0.026	1.82

Table 6 Photometry of 28978 Ixion (2001 KX_{76}); 2010 May. All the observations in the R filter; differential magnitudes are used.

Julian date	Mag
2455327.7814	1.099±0.056
2455327.7913	1.091±0.039
2455327.7997	1.069±0.049
2455327.8198	0.981±0.053
2455327.8297	1.048±0.047
2455327.8387	1.008±0.049
2455327.8723	1.028±0.070
2455327.8897	1.009±0.062
2455327.8982	0.997±0.052
2455327.9128	0.993±0.037
2455327.9150	0.988±0.041
2455327.9234	1.000±0.037
2455328.8044	0.978±0.049
2455328.8132	0.971±0.050
2455328.8241	1.052±0.052
2455328.8329	1.064±0.054
2455328.8419	1.011±0.049
2455328.8504	0.985±0.043
2455328.8588	1.067±0.050
2455328.8672	1.068±0.051
2455328.8840	1.026±0.060
2455328.8925	1.010±0.050
2455328.9177	1.062±0.069
2455328.9261	0.982±0.059
2455328.9346	0.995±0.053
2455328.9431	1.005±0.051
2455328.9515	1.029±0.052
2455328.9599	1.050±0.066
2455328.9683	1.027±0.061
2455328.9767	1.087±0.044
2455328.9852	1.051±0.050
2455328.9959	1.011±0.074
2455329.0164	0.986±0.050
2455329.0263	1.003±0.049
2455329.0347	1.037±0.049
2455329.0431	1.090±0.055
2455329.0516	1.064±0.047
2455329.0600	1.035±0.053
2455329.0685	0.979±0.052

with an albedo of 23±2% (Fornasier et al. 2013). Rabinowitz et al. (2007) give a value of 13.188 h for the rotational period of this object. Fornasier et al. (2013) suggest 10.47 h based on Thirouin et al. (2010) that gives an amplitude of 0.04±0.01 mag; a similar estimate is also given in Ortiz et al. (2006). Orcus has a known companion, Vanth, whose mass is comparable to that of the primary (Brown et al. 2010); its diameter is estimated to be 276±17 km (Fornasier et al. 2013). This may induce tidally locked rotation in the pair and Ortiz et al. (2011) have found possible evidence of this in the form of a photometric variability with a period of 9.7±0.3 days. Orcus was observed in 2010 May (see Tables 7 and 17) and again in 2011 January (see Tables 8 and 18) when it was in Sextans with the same equipment used for the previous four objects. The average geocentric distance of Orcus during the first observing run was $\bar{\Delta}$ = 47.73 AU, the average heliocentric distance was $\bar{r}$=47.90 AU, and the average phase angle (Earth–Orcus–Sun angle) was $\bar{\alpha} = 1.^{\circ}2$; the respective values for the second observing run were 47.29 AU, 47.92 AU and $0.^{\circ}9$. The periodogram in Fig. 5, middle panel, results from the analysis of the second run and shows several minima. Our best fit for the rotational period is P = 11.9±0.5 h (or a frequency of 0.084±0.004 rotations per hour). Unfortunately, the light-curve is rather flat and incomplete; it resembles those in figs. 18 and 19 in Sheppard (2007) that show an amplitude < 0.03 mag. The probability that there is no period with value P is > 90%. The light-curve of Orcus in Fig. 5, bottom panel, represents the data from the top panel phased with the best-fit period and exhibits a photometric amplitude of ∼0.05 which is similar in value to the error bars and also to the values cited in the literature. Small amplitude light-curves are characteristic of spherical objects with featureless surfaces and/or those observed under a nearly pole-on viewing geometry.

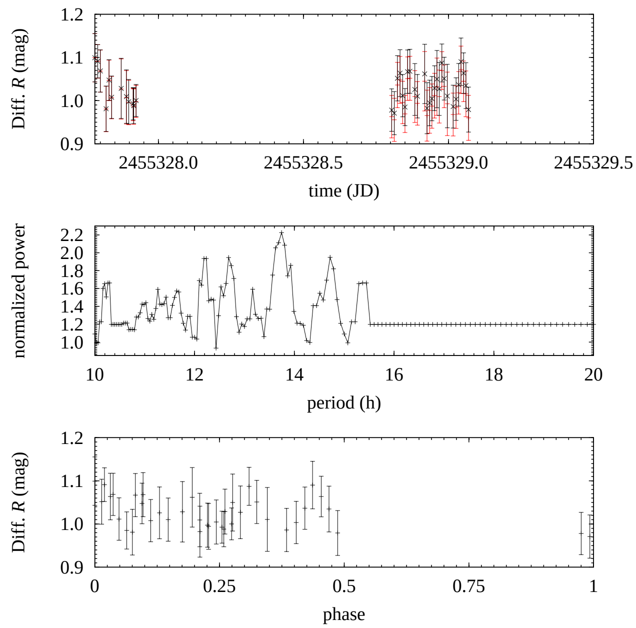

Fig. 4 Same as Fig. 1 but for Ixion, data obtained in 2010 May; 4×39 test frequencies. The lowest value of the normalized power corresponds to a rotation period of 12.4±0.3 h or a frequency of 0.080±0.002 cycles/h with a false alarm probability < 2%. The bottom panel shows the rotational light-curve of Ixion phased to a period of 12.4 h.

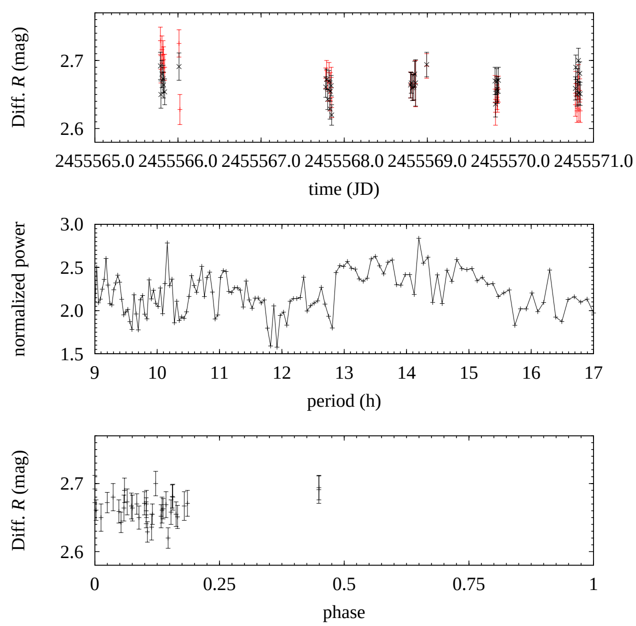

Fig. 5 Same as Fig. 1 but for Orcus, data obtained in 2011 January; 4×36 test frequencies. The lowest value of the normalized power corresponds to a rotation period of 11.9±0.5 h or a frequency of 0.084±0.004 cycles/h with a false alarm probability > 90%. The bottom panel shows the rotational light-curve of Orcus phased to a period of 11.9 h.

8 Discussion and conclusions

We have collected and analysed R-band photometric data for two Centaurs and three TNOs. In principle, our analysis confirms the published values of the rotational periods of Chiron, Chariklo, and Huya; the photometric amplitudes found are, in general, consistent with those quoted in the literature. These also exhibit notable dispersions, in particular those of Chiron. This may hint at changing surface features or, perhaps, chaotic rotation. Both Ixion and Orcus show behaviour compatible with no variability within the photometric uncertainties. Assuming that the data are reliable, lack of brightness variation may have its origin in slow spin, being viewed nearly pole-on, and/or round shape. In general, our rotational period results could be uncertain by a few tens of percent as they are based on less than full coverage of the light-curve. As for the overall rotational properties of Centaurs and TNOs, the extensive analysis in Thirouin et al. (2014) shows that single TNOs tend to spin faster than binaries. On the other hand, resonant TNOs (Plutinos in particular) are less prone to suffer planetary close encounters, such dynamical events may alter the rotational properties of Centaurs that are more likely to experience tidal interactions with the Jovian planets. In this context, the current values of the rotational periods of Chiron and Chariklo may not be primordial.

Visual inspection and measurements of the FWHM of the objects studied here and neighbouring star images did not reveal the presence of a coma around them. As an example, Fig. 6 compares the brightness profile of Chiron (first run) with that of a scaled background star. Their profiles are indistinguishable in all directions. Since the radial profile of Chiron is basically identical to that of the comparison stars, we conclude that a coma around Chiron was not present or it was well beyond our detection limit (order of 27.18 mag/arcsec^2) —if present at all. The absence of a detectable coma is compatible with the results in Fornasier et al. (2013). In order to constrain the possible presence of a coma, we use the relation given by Jewitt & Danielson (1984)

$$\Sigma(\phi) = m(\phi) + 2.5 \log(2\pi\phi^2)\,, \tag{4}$$

where $m(\phi)$ is the total magnitude of the coma inside a circle of radius ϕ in arcsec and $\Sigma(\phi)$ is the surface brightness at projected radius ϕ. The upper limit to the surface brightness of a hypothetical coma around the object at $\phi = 2\farcs175$ (almost double the seeing) can be set to be 27.18 mag/arcsec^2 as $m(2\farcs175) > 20$ mag in R. This is 3.49 mag fainter (factor of 25) than the limiting value for a single frame as 25 of them were coadded; for a SNR of 10 the limiting magnitude is 20 mag. Consistently, presence of candidate satellites or comoving wide companions brighter than 23.5 mag in R can also be discarded. Similar results have been obtained for the other objects. Modelling the dust production rate for Chiron or Chariklo is outside the scope of this work. The orbital solutions derived from the acquired astrometry (see Appendix A) are compatible with those already available from the JPL Small-Body Database, the MPC data server, or the AstDyS information service.

Acknowledgements We thank the anonymous referee for her/his constructive and helpful reports. M.

Table 7 Photometry of 90482 Orcus (2004 DW); 2010 May. All the observations in the R filter; differential magnitudes are used.

Julian date	A.M.	Mag	α(°)
2455327.4600	1.09	0.484±0.017	1.19
2455327.4684	1.09	0.506±0.016	1.19
2455327.4769	1.09	0.513±0.017	1.19
2455327.4854	1.10	0.536±0.014	1.19
2455327.4938	1.10	0.511±0.015	1.19
2455327.5028	1.12	0.524±0.017	1.19
2455327.5112	1.13	0.525±0.017	1.19
2455327.5196	1.15	0.496±0.013	1.19
2455327.5280	1.17	0.495±0.012	1.19
2455327.5364	1.20	0.521±0.013	1.19
2455327.5468	1.23	0.535±0.015	1.19
2455327.5552	1.27	0.527±0.013	1.19
2455327.5637	1.32	0.529±0.013	1.19
2455327.5721	1.37	0.515±0.011	1.19
2455327.5862	1.47	0.527±0.014	1.19
2455327.5947	1.54	0.547±0.015	1.19
2455327.6031	1.62	0.545±0.015	1.19

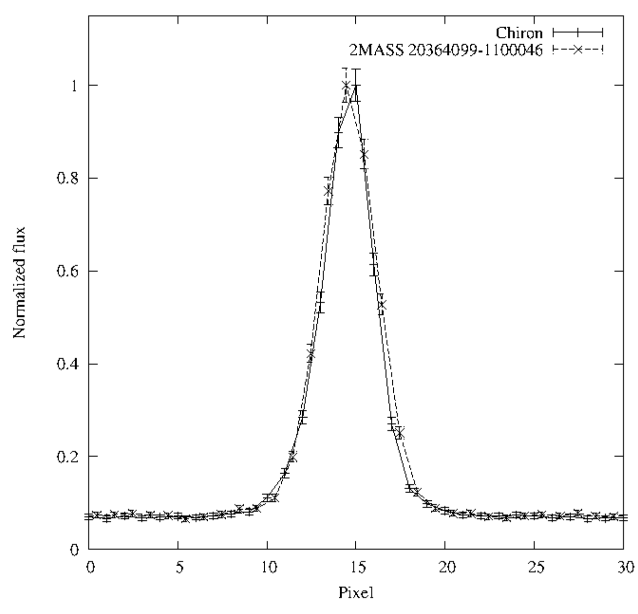

Fig. 6 The brightness profile of 2060 Chiron and that of a scaled background star (2MASS 20364099-1100046, B = 18.27, V = 17.17, R = 17.23) illustrate the stellar appearance of the Centaur.

G. and G. C. express their gratitude to S. Ortolani and S. Marchi for many useful discussions and advice. We thank R. Mateluna and L. Jílková for their help with the observations. In preparation of this paper, we made use of the NASA Astrophysics Data System, the ASTRO-PH e-print server, the JPL Small-Body Database, the MPC data server, and the AstDyS information service.

Table 8 Photometry of 90482 Orcus (2004 DW); 2011 January. All the observations in the R filter; differential magnitudes are used.

Julian date	A.M.	Mag	$\alpha(°)$
2455565.7892	1.10	2.729±0.020	0.93
2455565.7954	1.09	2.687±0.020	0.93
2455565.8074	1.08	2.716±0.020	0.93
2455565.8127	1.08	2.552±0.025	0.93
2455565.8214	1.08	2.709±0.020	0.93
2455565.8266	1.08	2.701±0.019	0.92
2455565.8404	1.09	2.690±0.019	0.92
2455566.0123	1.09	2.725±0.020	0.92
2455566.0234	1.10	2.628±0.022	0.92
2455566.0284	1.11	2.804±0.029	0.92
2455567.7775	1.11	2.674±0.015	0.90
2455567.7886	1.09	2.685±0.015	0.90
2455567.8023	1.08	2.655±0.015	0.90
2455567.8180	1.08	2.682±0.015	0.90
2455567.8286	1.08	2.641±0.015	0.90
2455567.8336	1.08	2.667±0.015	0.90
2455567.8442	1.10	2.675±0.015	0.90
2455567.8492	1.10	2.631±0.015	0.90
2455568.7987	1.08	2.664±0.019	0.89
2455568.8062	1.08	2.667±0.015	0.89
2455568.8209	1.08	2.660±0.019	0.89
2455568.9929	1.08	2.692±0.018	0.89
2455568.8367	1.09	2.661±0.019	0.89
2455568.8474	1.10	2.680±0.019	0.89
2455568.8588	1.12	2.666±0.034	0.89
2455569.8146	1.08	2.658±0.020	0.88
2455569.8198	1.08	2.624±0.019	0.88
2455569.8341	1.09	2.657±0.019	0.88
2455569.8391	1.10	2.646±0.018	0.88
2455569.8442	1.10	2.642±0.018	0.88
2455569.8555	1.12	2.658±0.019	0.88
2455570.7807	1.09	2.635±0.017	0.87
2455570.7863	1.09	2.666±0.018	0.87
2455570.8007	1.08	2.626±0.017	0.87
2455570.8061	1.08	2.647±0.017	0.87
2455570.8174	1.08	2.676±0.018	0.87
2455570.8227	1.08	2.628±0.017	0.87
2455570.8339	1.09	2.656±0.017	0.87
2455570.8391	1.10	2.626±0.017	0.87

References

Barucci, M.A., Belskaya, I.N., Fulchignoni, M., Birlan, M.: Astron. J. **130**, 1291 (2005)

Batygin, K., Brown, M.E.: Astron. J. **151**, 22 (2016)

Belskaya, I.N., Bagnulo, S., Barucci, M.A., Muinonen, K., Tozzi, G.P., Fornasier, S., Kolokolova, L.: Icarus **210**, 472 (2010)

Braga-Ribas, F., et al.: Nature **508**, 72 (2014)

Brown, M.E., Ragozzine, D., Stansberry, J., Fraser, W.C.: Astron. J. **139**, 2700 (2010)

Bus, S.J., Bowell, E., Harris, A.W., Hewitt, A.V.: Icarus **77**, 223 (1989)

Carraro, G.: Astron. J. **137**, 3089 (2009)

Carraro, G., Maris, M., Bertin, D., Parisi, M.G.: Astron. Astrophys. **460**, L39 (2006)

Clarke, D.: Astron. Astrophys. **386**, 763 (2002)

de la Fuente Marcos, C., de la Fuente Marcos, R.: Mon. Not. R. Astron. Soc. **443**, L59 (2014)

de la Fuente Marcos, C., de la Fuente Marcos, R., Aarseth, S.J.: Mon. Not. R. Astron. Soc. **446**, 1867 (2015)

Di Sisto, R.P., Brunini, A.: Icarus **190**, 224 (2007)

Duffard, R., et al.: Astron. Astrophys. **568**, A79 (2014)

Dworetsky, M.M.: Mon. Not. R. Astron. Soc. **203**, 917 (1983)

Fornasier, S., et al.: Astron. Astrophys. **555**, A15 (2013)

Fornasier, S., et al.: Astron. Astrophys. **568**, L11 (2014)

Fulchignoni, M., Belskaya, I.N., Barucci, M.A., de Sanctis, M.C., Doressoundiram, A.: In: Barucci, M.A., Boehnhardt, H., Cruikshank, D.P., Morbidelli, A., (eds.) The Solar System Beyond Neptune. p. 181. University of Arizona Press, Tucson (2008)

Galiazzo, M.: Masters Thesis, Università degli Studi di Padova, Italy (2009)

Galiazzo, M., Carruba, V., Wiegert, P.: IAU General Assembly, Meeting #29, id. 2252424 (2015)

Gladman, B., Marsden, B.G., Vanlaerhoven, C.: In: Barucci, M.A., Boehnhardt, H., Cruikshank, D.P., Morbidelli, A., (eds.) The Solar System Beyond Neptune. p. 43. University of Arizona Press, Tucson (2008)

Gladman, B., et al.: Astron. J. **144**, 23 (2012)

Hainaut, O.R., Delsanti, A.C.: Astron. Astrophys. **389**, 641 (2002)

Hamuy, M., et al.: Publ. Astron. Soc. Pac. **118**, 2 (2006)

Jewitt, D.: Astron. J. **137**, 4296 (2009)

Jewitt, D., Danielson, G.E.: Icarus **60**, 435 (1984)

Jewitt, D., Luu, J.: Nature **362**, 730 (1993)

Lacerda, P., Luu, J.: Astron. J. **131**, 2314 (2006)

Lafler, J., Kinman, T.D.: Astrophys. J. Suppl. Ser. **11**, 216 (1965)

Landolt, A.U.: Astron. J. **104**, 372 (1992)
Lang, D., Hogg, D.W., Mierle, K., Blanton, M., Roweis, S.: Astron. J. **139**, 1782 (2010)
Lellouch, E., et al.: Astron. Astrophys. **557**, A60 (2013)
Levison, H., Duncan, M.: Icarus **127**, 13 (1997)
Levison, H., Dones, L., Duncan, M.: Astron. J. **121**, 2253 (2001)
Lorin, O., Rousselot, P.: Mon. Not. R. Astron. Soc. **376**, 881 (2007)
Luu, J.X., Jewitt, D.C.: Astron. J. **100**, 913 (1990)
Marcialis, R.L., Buratti, B.J.: Icarus **104**, 234 (1993)
Naoz, S., Perets, H.B., Ragozzine, D.: Astrophys. J. **719**, 1775 (2010)
Ortiz, J.L., Gutiérrez, P.J., Casanova, V., Sota, A.: Astron. Astrophys. **407**, 1149 (2003)
Ortiz, J.L., Gutiérrez, P.J., Santos-Sanz, P., Casanova, V., Sota, A.: Astron. Astrophys. **447**, 1131 (2006)
Ortiz, J.L., et al.: Astron. Astrophys. **525**, 31 (2011)
Ortiz, J.L., et al.: Astron. Astrophys. **576**, A18 (2015)
Parker, A.H.: Ph.D. Thesis, University of Victoria, Canada (2011)
Parker, A.H., Kavelaars, J.J., Petit, J.-M., Jones, L., Gladman, B., Parker, J.: Astrophys. J. **743**, 1 (2011)
Press, W.H., Teukolsky, S.A., Vetterling, W.T., Flannery, B.P.: Numerical Recipes: The Art of Scientific Computing, 3rd Edition. Cambridge University Press, Cambridge (2007)
Rabinowitz, D.L., Schaefer, B.E., Tourtellotte, S.W.: Astron. J. **133**, 26 (2007)
Romanishin, W., Tegler, S.C.: Icarus **179**, 523 (2005)
Rousselot, P., Petit, J.: AAS, DPS meeting #42, #40.19 (2010)
Ruprecht, J.D., et al.: Icarus **252**, 271 (2015)
Sheppard, S.S.: Astron. J. **134**, 787 (2007)
Sheppard, S.S., Lacerda, P., Ortiz, J.L.: In: Barucci, M.A., Boehnhardt, H., Cruikshank, D.P., Morbidelli, A., (eds.) The Solar System Beyond Neptune. p. 129. University of Arizona Press, Tucson (2008)
Stetson, P.B.: Publ. Astron. Soc. Pac. **99**, 191 (1987)
Thirouin, A., Ortiz, J.L., Duffard, R., Santos-Sanz, P., Aceituno, F.J., Morales, N.: Astron. Astrophys. **522**, A93 (2010)
Thirouin, A., Noll, K.S., Ortiz, J.L., Morales, N.: Astron. Astrophys. **563**, A3 (2014)
Trujillo, C.A., Sheppard, S.S.: Nature **507**, 471 (2014)
Wall, J.V., Jenkins, C.R.: Practical Statistics for Astronomers, 2nd Edition. Cambridge University Press, Cambridge (2012)
Walsh, K.J.: Earth, Moon, and Planets **105**, 193 (2009)

This 2-column preprint was prepared with the AAS LaTeX macros v5.2.

A Astrometry of 2060 Chiron (1977 UB), 10199 Chariklo (1997 CU_{26}), 38628 Huya (2000 EB_{173}), 28978 Ixion (2001 KX_{76}), and 90482 Orcus (2004 DW)

Table 9 Observations of 2060 Chiron (1977 UB) over interval 2006 June 26.298391 – 28.313276. During this observing run, Chiron was in Capricornus. See also Table 1.

Date (UT)	RA(J2000) ($^{h}:^{m}:^{s}$)	Dec(J2000) ($^{\circ}:':''$)	Filter
2006 6 26.298391	20:36:46.81	−11:00:29.8	*B*
2006 6 26.305822	20:36:46.72	−11:00:30.1	*R*
2006 6 26.311991	20:36:46.67	−11:00:30.3	*V*
2006 6 26.318206	20:36:46.61	−11:00:30.4	*I*
2006 6 26.324410	20:36:46.54	−11:00:30.5	*R*
2006 6 26.357975	20:36:46.18	−11:00:31.0	*R*
2006 6 26.364005	20:36:46.12	−11:00:31.2	*R*
2006 6 26.370023	20:36:46.04	−11:00:31.4	*R*
2006 6 26.376053	20:36:45.99	−11:00:31.6	*R*
2006 6 26.382084	20:36:45.93	−11:00:31.8	*R*
2006 6 26.389491	20:36:45.86	−11:00:31.8	*B*
2006 6 26.397037	20:36:45.78	−11:00:31.9	*R*
2006 6 26.403067	20:36:45.69	−11:00:31.9	*R*
2006 6 26.410428	20:36:45.64	−11:00:32.4	*B*
2006 6 28.189248	20:36:26.98	−11:01:13.5	*R*
2006 6 28.195278	20:36:26.92	−11:01:13.7	*R*
2006 6 28.201296	20:36:26.84	−11:01:13.8	*R*
2006 6 28.224491	20:36:26.57	−11:01:14.5	*R*
2006 6 28.230521	20:36:26.51	−11:01:14.7	*R*
2006 6 28.236540	20:36:26.43	−11:01:15.0	*R*
2006 6 28.258970	20:36:26.20	−11:01:15.3	*R*
2006 6 28.265000	20:36:26.14	−11:01:15.5	*R*
2006 6 28.271030	20:36:26.07	−11:01:15.8	*R*
2006 6 28.277049	20:36:26.00	−11:01:16.0	*R*
2006 6 28.283079	20:36:25.94	−11:01:16.2	*R*
2006 6 28.289167	20:36:25.87	−11:01:16.2	*R*
2006 6 28.294503	20:36:25.81	−11:01:16.4	*R*
2006 6 28.301227	20:36:25.74	−11:01:16.5	*R*
2006 6 28.307246	20:36:25.70	−11:01:16.6	*R*
2006 6 28.313276	20:36:25.59	−11:01:16.8	*R*

Table 10 Observations of 2060 Chiron (1977 UB) over interval 2011 July 30.217766 – August 06.393033. During this observing run, Chiron was in Aquarius. All the observations in the R filter. See also Table 2.

Date (UT)	RA(J2000) (^{h}:^{m}:^{s})	Dec(J2000) (°:′:″)
2011 7 30.217766	22:15:08.78	−04:16:07.4
2011 7 30.226655	22:15:08.68	−04:16:07.8
2011 7 30.238704	22:15:08.57	−04:16:08.2
2011 7 30.250452	22:15:08.43	−04:16:09.0
2011 7 30.261412	22:15:08.35	−04:16:09.4
2011 7 30.272199	22:15:08.24	−04:16:09.9
2011 7 30.283102	22:15:08.12	−04:16:10.6
2011 7 30.293854	22:15:08.02	−04:16:11.2
2011 7 30.304618	22:15:07.91	−04:16:11.6
2011 7 30.315347	22:15:07.82	−04:16:12.4
2011 7 30.329169	22:15:07.68	−04:16:12.8
2011 7 30.340347	22:15:07.58	−04:16:13.2
2011 7 30.350047	22:15:07.47	−04:16:13.8
2011 7 30.358658	22:15:07.42	−04:16:14.1
2011 7 30.367060	22:15:07.30	−04:16:14.7
2011 7 30.375475	22:15:07.20	−04:16:15.0
2011 7 30.383889	22:15:07.15	−04:16:15.5
2011 7 30.392292	22:15:07.04	−04:16:15.8
2011 7 30.400706	22:15:06.96	−04:16:16.2
2011 7 30.409144	22:15:06.87	−04:16:16.5
2011 7 30.417558	22:15:06.80	−04:16:17.1
2011 8 02.194271	22:14:39.86	−04:18:31.1
2011 8 02.202766	22:14:39.77	−04:18:31.7
2011 8 02.212813	22:14:39.67	−04:18:32.3
2011 8 02.223380	22:14:39.57	−04:18:32.8
2011 8 02.246100	22:14:39.35	−04:18:33.8
2011 8 02.258449	22:14:39.21	−04:18:34.4
2011 8 02.270695	22:14:39.08	−04:18:35.4
2011 8 02.292616	22:14:38.86	−04:18:36.5
2011 8 02.305799	22:14:38.72	−04:18:37.0
2011 8 02.316470	22:14:38.63	−04:18:37.6
2011 8 02.360116	22:14:38.18	−04:18:39.6
2011 8 02.371898	22:14:38.06	−04:18:40.4
2011 8 02.380336	22:14:37.99	−04:18:40.8
2011 8 02.388762	22:14:37.88	−04:18:41.3
2011 8 02.397188	22:14:37.80	−04:18:41.8
2011 8 02.405614	22:14:37.70	−04:18:42.2
2011 8 02.414040	22:14:37.62	−04:18:42.7
2011 8 06.179375	22:13:59.81	−04:21:57.2
2011 8 06.187778	22:13:59.71	−04:21:57.7
2011 8 06.197523	22:13:59.61	−04:21:58.3
2011 8 06.205926	22:13:59.55	−04:21:58.8
2011 8 06.214317	22:13:59.43	−04:21:59.2
2011 8 06.222847	22:13:59.34	−04:21:59.7
2011 8 06.231239	22:13:59.22	−04:21:59.9
2011 8 06.239641	22:13:59.13	−04:22:00.4
2011 8 06.265116	22:13:58.96	−04:22:01.7
2011 8 06.273600	22:13:58.84	−04:22:02.4
2011 8 06.281991	22:13:58.74	−04:22:02.8
2011 8 06.290394	22:13:58.64	−04:22:03.2
2011 8 06.314792	22:13:58.39	−04:22:04.3
2011 8 06.325417	22:13:58.27	−04:22:04.8
2011 8 06.333854	22:13:58.19	−04:22:05.2
2011 8 06.342246	22:13:58.12	−04:22:05.8
2011 8 06.350695	22:13:58.03	−04:22:06.2
2011 8 06.359097	22:13:57.94	−04:22:06.8
2011 8 06.367489	22:13:57.85	−04:22:07.3
2011 8 06.376146	22:13:57.77	−04:22:07.7
2011 8 06.384560	22:13:57.68	−04:22:08.1
2011 8 06.393033	22:13:57.59	−04:22:08.7
2011 8 06.401435	22:13:57.50	−04:22:09.0

Table 11 Observations of 2060 Chiron (1977 UB) over interval 2006 May 19.383990 – 22.438617. During this observing run, Chiron was in Aquarius.

Date (UT)	RA(J2000) (^{h}:^{m}:^{s})	Dec(J2000) ($^{\circ}$:$'$:$''$)	Filter
2006 5 19.383990	20:40:46.42	−11:00:36.5	R
2006 5 19.389247	20:40:46.41	−11:00:36.2	V
2006 5 19.394501	20:40:46.39	−11:00:36.2	R
2006 5 19.407375	20:40:46.39	−11:00:35.9	R
2006 5 19.412628	20:40:46.37	−11:00:35.9	I
2006 5 19.417883	20:40:46.34	−11:00:35.6	R
2006 5 19.423152	20:40:46.33	−11:00:35.5	V
2006 5 19.428409	20:40:46.32	−11:00:35.4	R
2006 5 19.441269	20:40:46.30	−11:00:35.1	R
2006 5 19.446528	20:40:46.28	−11:00:35.0	I
2006 5 22.426946	20:40:40.18	−10:59:32.1	R
2006 5 22.432782	20:40:40.18	−10:59:31.9	V
2006 5 22.438617	20:40:40.16	−10:59:31.8	R

Table 12 Observations of Chariklo over interval 2006 June 27.950405 – 30.113403. See also Table 3. During this observing run, Chariklo was in Hydra.

Date (UT)	RA(J2000) (^{h}:^{m}:^{s})	Dec(J2000) ($^{\circ}$:$'$:$''$)	Filter
2006 6 27.950405	12:24:30.52	−28:28:12.9	R
2006 6 27.956100	12:24:30.54	−28:28:12.5	V
2006 6 27.962315	12:24:30.57	−28:28:12.2	R
2006 6 27.968484	12:24:30.59	−28:28:11.6	V
2006 6 27.974676	12:24:30.62	−28:28:11.3	R
2006 6 27.980833	12:24:30.65	−28:28:10.7	I
2006 6 27.987072	12:24:30.68	−28:28:10.3	R
2006 6 28.039294	12:24:30.93	−28:28:06.2	R
2006 6 28.045313	12:24:30.96	−28:28:05.8	R
2006 6 28.078819	12:24:31.12	−28:28:03.2	R
2006 6 28.084850	12:24:31.14	−28:28:02.7	R
2006 6 28.117986	12:24:31.31	−28:28:00.1	R
2006 6 28.973970	12:24:35.84	−28:26:55.3	R
2006 6 28.989641	12:24:35.93	−28:26:53.9	R
2006 6 29.953565	12:24:41.27	−28:25:42.5	R
2006 6 29.958426	12:24:41.30	−28:25:42.1	R
2006 6 29.963299	12:24:41.32	−28:25:41.8	R
2006 6 30.010891	12:24:41.58	−28:25:38.3	R
2006 6 30.035081	12:24:41.70	−28:25:36.7	R
2006 6 30.060914	12:24:41.85	−28:25:34.8	R
2006 6 30.086921	12:24:41.99	−28:25:32.8	R
2006 6 30.113403	12:24:42.15	−28:25:30.7	R

Table 13 Observations of Chariklo over interval 2011 July 30.043623 – August 06.162685. During this observing run, Chariklo was in Lupus. All the observations in the R filter. See also Table 4.

Date (UT)	RA(J2000) (^{h}:^{m}:^{s})	Dec(J2000) ($^{\circ}$:$'$:$''$)
2011 7 30.043623	15:29:12.14	−40:01:58.6
2011 7 30.052083	15:29:12.13	−40:01:57.7
2011 7 30.060567	15:29:12.13	−40:01:56.9
2011 7 30.074074	15:29:12.09	−40:01:55.4
2011 7 30.084757	15:29:12.09	−40:01:53.9
2011 7 30.100174	15:29:12.08	−40:01:52.8
2011 7 30.111632	15:29:12.07	−40:01:51.6
2011 7 30.122697	15:29:12.06	−40:01:50.6
2011 7 30.134063	15:29:12.06	−40:01:49.5
2011 7 30.145208	15:29:12.05	−40:01:48.2
2011 7 30.156111	15:29:12.05	−40:01:47.1
2011 8 01.994016	15:29:12.71	−39:57:04.5
2011 8 02.002535	15:29:12.72	−39:57:03.7
2011 8 02.010972	15:29:12.72	−39:57:02.9
2011 8 02.019398	15:29:12.73	−39:57:02.0
2011 8 02.027824	15:29:12.73	−39:57:01.2
2011 8 02.036250	15:29:12.73	−39:57:00.4
2011 8 02.044699	15:29:12.73	−39:56:59.5
2011 8 02.053137	15:29:12.74	−39:56:58.8
2011 8 02.061563	15:29:12.74	−39:56:57.9
2011 8 02.069988	15:29:12.74	−39:56:56.9
2011 8 02.078426	15:29:12.75	−39:56:56.2
2011 8 02.086863	15:29:12.75	−39:56:55.3
2011 8 02.095289	15:29:12.76	−39:56:54.5
2011 8 02.103727	15:29:12.77	−39:56:53.7
2011 8 02.116771	15:29:12.77	−39:56:52.4
2011 8 02.126400	15:29:12.77	−39:56:51.5
2011 8 02.135914	15:29:12.78	−39:56:50.5
2011 8 02.144352	15:29:12.79	−39:56:49.6
2011 8 02.153252	15:29:12.79	−39:56:48.7
2011 8 02.161690	15:29:12.79	−39:56:47.8
2011 8 02.170139	15:29:12.80	−39:56:47.0
2011 8 02.178553	15:29:12.81	−39:56:46.2
2011 8 05.009792	15:29:16.44	−39:52:10.7
2011 8 05.018194	15:29:16.45	−39:52:09.9
2011 8 05.026620	15:29:16.47	−39:52:09.1
2011 8 05.036678	15:29:16.49	−39:52:08.3
2011 8 05.045590	15:29:16.50	−39:52:07.3
2011 8 05.073171	15:29:16.54	−39:52:04.5
2011 8 05.081586	15:29:16.55	−39:52:03.7
2011 8 05.119340	15:29:16.60	−39:52:00.0
2011 8 05.127755	15:29:16.62	−39:51:59.2
2011 8 05.136169	15:29:16.63	−39:51:58.4
2011 8 05.144676	15:29:16.65	−39:51:57.8
2011 8 05.153090	15:29:16.66	−39:51:57.2
2011 8 06.034132	15:29:18.44	−39:50:32.6
2011 8 06.043657	15:29:18.46	−39:50:31.7
2011 8 06.053125	15:29:18.47	−39:50:30.8
2011 8 06.061586	15:29:18.49	−39:50:29.9
2011 8 06.069988	15:29:18.51	−39:50:29.2
2011 8 06.078380	15:29:18.52	−39:50:28.3
2011 8 06.086834	15:29:18.54	−39:50:27.5
2011 8 06.095231	15:29:18.55	−39:50:26.7
2011 8 06.103634	15:29:18.57	−39:50:25.9
2011 8 06.112106	15:29:18.58	−39:50:25.1
2011 8 06.120498	15:29:18.60	−39:50:24.3
2011 8 06.128900	15:29:18.61	−39:50:23.5
2011 8 06.137431	15:29:18.63	−39:50:22.7
2011 8 06.145828	15:29:18.65	−39:50:21.9
2011 8 06.154236	15:29:18.67	−39:50:21.1
2011 8 06.162685	15:29:18.69	−39:50:20.3

Table 14 Observations of 38628 Huya (2000 EB_{173}) over interval 2006 June 27.994178 – 30.149815. During this observing run, Huya was in Virgo. See also Table 5.

Date (UT)	RA(J2000) (^{h}:^{m}:^{s})	Dec(J2000) ($^{\circ}$:$'$:$''$)	Filter
2006 6 27.994178	14:12:43.60	−01:36:27.2	*R*
2006 6 28.000347	14:12:43.58	−01:36:27.3	*V*
2006 6 28.006551	14:12:43.55	−01:36:27.3	*R*
2006 6 28.012813	14:12:43.55	−01:36:27.6	*R*
2006 6 28.019028	14:12:43.53	−01:36:27.6	*R*
2006 6 28.052604	14:12:43.47	−01:36:27.8	*R*
2006 6 28.058831	14:12:43.44	−01:36:27.8	*R*
2006 6 28.092060	14:12:43.37	−01:36:28.0	*R*
2006 6 28.098079	14:12:43.34	−01:36:28.5	*R*
2006 6 28.124873	14:12:43.30	−01:36:28.2	*R*
2006 6 28.131030	14:12:43.29	−01:36:28.3	*V*
2006 6 28.137211	14:12:43.29	−01:36:28.4	*I*
2006 6 28.143403	14:12:43.25	−01:36:28.6	*R*
2006 6 28.149433	14:12:43.23	−01:36:28.6	*R*
2006 6 29.967211	14:12:39.76	−01:36:39.7	*R*
2006 6 29.971181	14:12:39.73	−01:36:40.2	*R*
2006 6 29.977211	14:12:39.70	−01:36:40.3	*R*
2006 6 29.983241	14:12:39.69	−01:36:40.3	*R*
2006 6 30.018438	14:12:39.64	−01:36:40.5	*R*
2006 6 30.043808	14:12:39.58	−01:36:40.8	*R*
2006 6 30.069086	14:12:39.51	−01:36:41.3	*R*
2006 6 30.095591	14:12:39.46	−01:36:41.5	*R*
2006 6 30.121945	14:12:39.43	−01:36:41.7	*R*
2006 6 30.149815	14:12:39.40	−01:36:42.1	*R*

Table 15 Observations of 28978 Ixion (2001 KX_{76}) over interval 2010 May 9.267685 – 12.396771. During this observing run, Ixion was in Ophiuchus. See also Table 6.

Date (UT)	RA(J2000) ($^{h:m:s}$)	Dec(J2000) ($^{\circ:\prime:\prime\prime}$)
2010 5 09.262489	17:00:21.57	−24:28:18.4
2010 5 09.267685	17:00:21.54	−24:28:18.2
2010 5 09.272616	17:00:21.53	−24:28:18.1
2010 5 09.277558	17:00:21.50	−24:28:18.0
2010 5 09.284294	17:00:21.46	−24:28:19.0
2010 5 09.292894	17:00:21.43	−24:28:17.7
2010 5 09.301459	17:00:21.39	−24:28:18.0
2010 5 09.311817	17:00:21.34	−24:28:18.1
2010 5 11.118172	17:00:12.79	−24:28:15.9
2010 5 11.128114	17:00:12.73	−24:28:15.8
2010 5 11.136540	17:00:12.68	−24:28:15.7
2010 5 11.144861	17:00:12.63	−24:28:15.9
2010 5 11.156586	17:00:12.60	−24:28:15.9
2010 5 11.166470	17:00:12.55	−24:28:15.9
2010 5 11.175510	17:00:12.50	−24:28:15.7
2010 5 11.183924	17:00:12.46	−24:28:15.7
2010 5 11.192327	17:00:12.43	−24:28:15.7
2010 5 11.200729	17:00:12.40	−24:28:15.6
2010 5 11.209144	17:00:12.34	−24:28:15.6
2010 5 11.217847	17:00:12.31	−24:28:15.6
2010 5 11.226551	17:00:12.25	−24:28:15.7
2010 5 11.234966	17:00:12.23	−24:28:15.9
2010 5 11.243368	17:00:12.19	−24:28:15.8
2010 5 11.251783	17:00:12.14	−24:28:15.7
2010 5 11.260197	17:00:12.10	−24:28:15.7
2010 5 11.269167	17:00:12.06	−24:28:15.6
2010 5 11.277581	17:00:12.00	−24:28:15.7
2010 5 11.285984	17:00:11.97	−24:28:15.6
2010 5 11.294398	17:00:11.92	−24:28:15.7
2010 5 11.302801	17:00:11.91	−24:28:15.9
2010 5 11.321621	17:00:11.81	−24:28:15.8
2010 5 11.330579	17:00:11.72	−24:28:15.7
2010 5 11.338993	17:00:11.66	−24:28:15.8
2010 5 11.347396	17:00:11.65	−24:28:15.8
2010 5 11.355810	17:00:11.62	−24:28:15.8
2010 5 11.364213	17:00:11.56	−24:28:15.8
2010 5 11.373021	17:00:11.50	−24:28:15.7
2010 5 11.381435	17:00:11.45	−24:28:15.7
2010 5 11.389954	17:00:11.42	−24:28:15.6
2010 5 11.398368	17:00:11.41	−24:28:15.6
2010 5 12.141204	17:00:07.84	−24:28:14.7
2010 5 12.149989	17:00:07.83	−24:28:14.6
2010 5 12.160891	17:00:07.78	−24:28:14.5
2010 5 12.169734	17:00:07.70	−24:28:14.5
2010 5 12.178704	17:00:07.69	−24:28:14.5
2010 5 12.187165	17:00:07.62	−24:28:14.5
2010 5 12.195567	17:00:07.61	−24:28:14.5
2010 5 12.203993	17:00:07.55	−24:28:14.6
2010 5 12.212396	17:00:07.52	−24:28:14.5
2010 5 12.220810	17:00:07.48	−24:28:14.5
2010 5 12.229294	17:00:07.44	−24:28:14.5
2010 5 12.237709	17:00:07.40	−24:28:14.5
2010 5 12.246123	17:00:07.35	−24:28:14.6
2010 5 12.254537	17:00:07.30	−24:28:14.5
2010 5 12.262940	17:00:07.27	−24:28:14.5
2010 5 12.271366	17:00:07.22	−24:28:14.5
2010 5 12.279861	17:00:07.16	−24:28:14.5
2010 5 12.288276	17:00:07.15	−24:28:14.4
2010 5 12.296678	17:00:07.10	−24:28:14.4
2010 5 12.305093	17:00:07.06	−24:28:14.4
2010 5 12.313507	17:00:06.98	−24:28:14.4
2010 5 12.322014	17:00:06.97	−24:28:14.4
2010 5 12.332732	17:00:06.90	−24:28:14.3
2010 5 12.341146	17:00:06.88	−24:28:14.3
2010 5 12.353172	17:00:06.78	−24:28:14.5
2010 5 12.363137	17:00:06.73	−24:28:14.5
2010 5 12.371551	17:00:06.69	−24:28:14.5
2010 5 12.379954	17:00:06.65	−24:28:14.6
2010 5 12.388357	17:00:06.60	−24:28:14.5
2010 5 12.396771	17:00:06.56	−24:28:14.5

Table 16 Observations of 28978 Ixion (2001 KX_{76}) over interval 2006 June 28.031296 – 30.257153. During this observing run, Ixion was in Ophiuchus.

Date (UT)	RA(J2000) (^{h}:^{m}:^{s})	Dec(J2000) ($^{\circ}$:$'$:$''$)
2006 6 28.025961	16:36:02.79	−22:06:19.4
2006 6 28.031296	16:36:02.75	−22:06:19.1
2006 6 28.065787	16:36:02.61	−22:06:19.1
2006 6 28.071806	16:36:02.58	−22:06:19.0
2006 6 28.105047	16:36:02.39	−22:06:18.5
2006 6 28.111077	16:36:02.36	−22:06:18.7
2006 6 28.156597	16:36:02.19	−22:06:18.3
2006 6 28.162801	16:36:02.13	−22:06:18.4
2006 6 28.169016	16:36:02.12	−22:06:18.5
2006 6 28.175232	16:36:02.08	−22:06:18.3
2006 6 28.181470	16:36:02.05	−22:06:18.4
2006 6 28.208438	16:36:01.94	−22:06:18.3
2006 6 28.213947	16:36:01.91	−22:06:18.4
2006 6 29.987709	16:35:53.81	−22:06:09.3
2006 6 29.991713	16:35:53.75	−22:06:09.2
2006 6 29.997743	16:35:53.74	−22:06:09.2
2006 6 30.003762	16:35:53.68	−22:06:09.2
2006 6 30.027107	16:35:53.60	−22:06:09.1
2006 6 30.052928	16:35:53.48	−22:06:09.0
2006 6 30.078287	16:35:53.37	−22:06:08.7
2006 6 30.104746	16:35:53.23	−22:06:08.7
2006 6 30.131412	16:35:53.09	−22:06:08.6
2006 6 30.159387	16:35:52.97	−22:06:08.7
2006 6 30.177928	16:35:52.90	−22:06:08.5
2006 6 30.196204	16:35:52.80	−22:06:08.5
2006 6 30.215648	16:35:52.71	−22:06:08.3
2006 6 30.236377	16:35:52.61	−22:06:08.0
2006 6 30.257153	16:35:52.52	−22:06:07.7

Table 17 Observations of 90482 Orcus (2004 DW) over interval 2010 May 10.963438 – 12.100394. During this observing run, Orcus was in Sextans. See also Table 7.

Date (UT)	RA(J2000) (^{h}:^{m}:^{s})	Dec(J2000) ($^{\circ}$:$'$:$''$)
2010 5 10.963438	09:42:04.42	−05:48:59.6
2010 5 10.988831	09:42:04.51	−05:48:59.7
2010 5 10.997269	09:42:04.54	−05:48:59.8
2010 5 11.014688	09:42:04.50	−05:48:58.0
2010 5 11.031505	09:42:04.49	−05:48:57.9
2010 5 11.050313	09:42:04.48	−05:48:57.4
2010 5 11.098172	09:42:04.47	−05:48:56.6
2010 5 11.106609	09:42:04.56	−05:48:56.8
2010 5 12.057917	09:42:04.74	−05:48:37.0
2010 5 12.083553	09:42:04.78	−05:48:36.8
2010 5 12.100394	09:42:04.84	−05:48:35.9

Table 18 Observations of 90482 Orcus (2004 DW) over interval 2011 January 04.31616 – 09.32441. During this observing run, Orcus was in Sextans. See also Table 8.

Date (UT)	RA(J2000) ($^{\rm h}$:$^{\rm m}$:$^{\rm s}$)	Dec(J2000) ($^\circ$:$'$:$''$)	Filter
2011 1 04.31616	09:51:50.11	−07:01:27.2	*B*
2011 1 05.31395	09:51:47.08	−07:01:30.9	*V*
2011 1 05.34266	09:51:46.97	−07:01:31.2	*R*
2011 1 06.27920	09:51:44.07	−07:01:34.3	*R*
2011 1 06.29004	09:51:44.07	−07:01:34.4	*R*
2011 1 06.33538	09:51:43.92	−07:01:34.4	*R*
2011 1 06.35095	09:51:43.87	−07:01:34.4	*R*
2011 1 07.33845	09:51:40.72	−07:01:37.1	*R*
2011 1 09.29526	09:51:34.40	−07:01:41.2	*B*
2011 1 09.32441	09:51:34.32	−07:01:41.2	*R*